# Vertical electrostatic force in MEMS cantilever IR sensor

Imen Rezadad, Javaneh Boroumand, Evan M. Smith, Ammar Alhasan, Robert E. Peale
University of Central Florida, Physics Department, Orlando, FL, 32816

## ABSTRACT

A MEMS cantilever IR detector that repetitively lifts from the surface under the influence of a saw-tooth electrostatic force, where the contact duty cycle is a measure of the absorbed IR radiation, is analyzed. The design is comprised of three parallel conducting plates. Fixed buried and surface plates are held at opposite potential. A moveable cantilever is biased the same as the surface plate. Calculations based on energy methods with position-dependent capacity and electrostatic induction coefficients demonstrate the upward sign of the force on the cantilever and determine the force magnitude. 2D finite element method calculations of the local fields confirm the sign of the force and determine its distribution across the cantilever. The upward force is maximized when the surface plate is slightly larger than the other two. The electrostatic repulsion is compared with Casimir sticking force to determine the maximum useful contact area. MEMS devices were fabricated and the vertical displacement of the cantilever was observed in a number of experiments. The approach may be applied also to MEMS actuators and micromirrors.

**Keywords:** MEMS, Electrostatic, Repulsive force, Cantilever, IR Sensor, Casimir Force, Finite element analysis

## 1. INTRODUCTION

One of the challenges in design and operation of MEMS devices is to overcome stiction of their parts to the substrate. Current techniques require adding extra lateral components to lift the device from the surface at the expense of lowering the fill factor [1,2]. Edwards [3] proposed a design to achieve an electrostatic force that lifts a cantilever up from the surface. In this design, the critical components are arranged vertically, so that high fill factor is achieved.

Our initial theoretical and experimental results for the Edwards design are currently under review for publication[4]. To summarize that manuscript, analytical calculation of the electrostatic force has demonstrated the upward sign of the force on the cantilever and the position-dependent magnitude of the force. The calculation was based on the energy method, which included the energy of the charge reservoirs necessary to maintain the various conductors at constant potential as the cantilever's position changes. These calculations used values for the coefficients of capacity and electrostatic induction, which depend on the geometry of the conductors and their relative positions. These coefficients were determined as a function of cantilever position using the 3D finite element method (FEM).

Additionally [4], direct observation of the cantilever displacement was made by video microscopy and by electrical sensing of electrically-controlled repetitive contact of the cantilever tip to the substrate surface. The device was fabricated according to Edwards's design. The process is described in references [5,6].

In this paper, we update our analytical calculation [4] to include the permittivity of the structural oxide, on which the conductors are deposited. Here we present 2D finite element method calculations to verify the sign of the force and to determine its distribution across the cantilever. Moreover, we vary the relative dimensions of the plates to optimize the design for maximum net upward force. We also compare electrostatic, elastic, and Casimir forces, where the latter is a contact force responsible for stiction.

## 2. ANALYTIC FORCE CALCULATION

The model consists of three parallel plates (Figure 1, left). The buried plate is fixed at depth d below the surface and is held at −V/2 potential. The surface plate is fixed at the surface and is held at +V/2. The cantilever is electrically connected to the surface plate and is free to move vertically.

Fig. 1 (right) present a scanning electron microscope image for one of our fabricated devices. The cantilever tip is in contact with a metal tip pad on the surface. This is the intended equilibrium "null position".
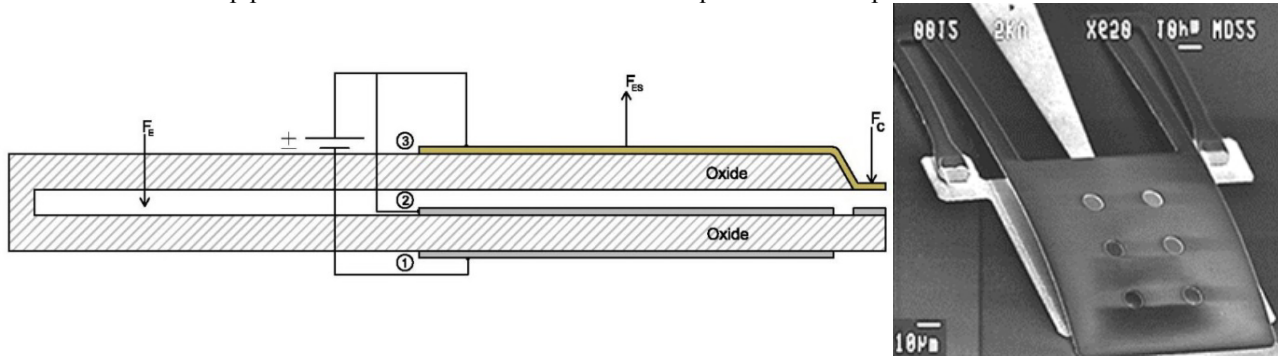


Figure 1. (left) Schematic of system. (right) Scanning electron microscope image of a fabricated device with 100 μm x 100 μm paddle.

The derivation of an analytic expression for the electrostatic force on the cantilever is presented in reference [4]. There, all plates were considered to be square and to have the same 18 μm x 18 μm dimensions. The permittivity of the oxide was ignored. Here we present results of a new calculation that includes the permittivity of the structural oxide (PECVD SiO$_2$), with new coefficients of capacity and electrostatic induction calculated by FEM (FastCap [7]). The expression for the force is [4]

$$F = \frac{V^2}{8}\left[-2\frac{\partial C_{12}}{\partial \zeta} - 2\frac{\partial C_{13}}{\partial \zeta} + 2\frac{\partial C_{23}}{\partial \zeta} + \frac{\partial C_{11}}{\partial \zeta} + \frac{\partial C_{22}}{\partial \zeta} + \frac{\partial C_{33}}{\partial \zeta}\right] \tag{1}$$

The coefficients in Eq. 1 are functions of the height of the cantilever metal above the surface metal, which we represent by the distance $\zeta$. Because of the structural oxide, the minimum value of $\zeta$ is 0.5 μm. These coefficients are plotted as a function of $\zeta$ in Figure 2 (left). Three of the coefficients have negligible derivative. Of the other three, the slope of $C_{23}$ is positive and exceeds in magnitude the negative slopes of $C_{22}$ and $C_{33}$ at every point. Hence, by Eq. (1) the electrostatic force is in the direction of increasing $\zeta$, i.e. upwards. The resulting force from Eq. 1 is compared with the calculation results that ignored oxide [4] in Fig. 2 (right). The effect of oxide is to increase the magnitude of the force by nearly 4x.
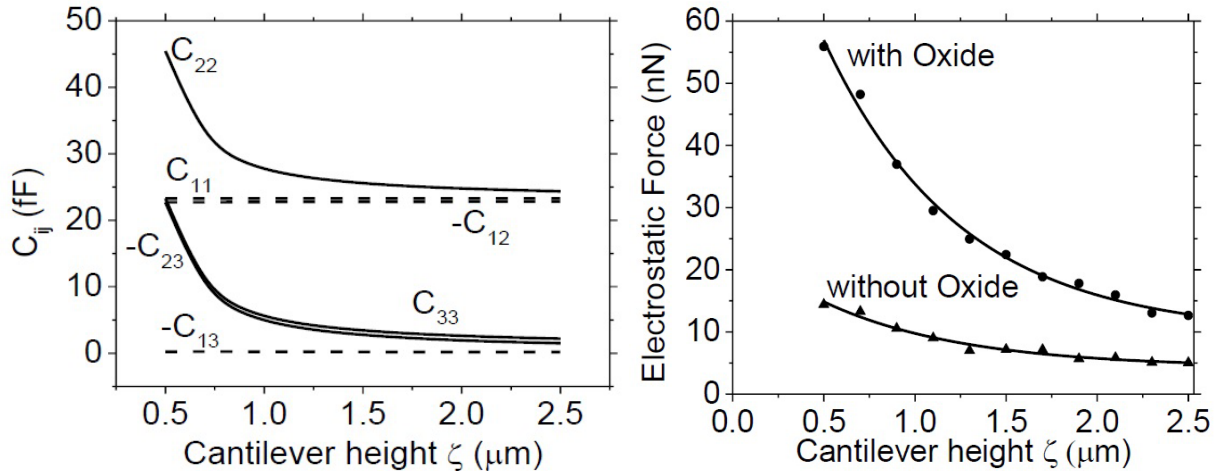
Figure 2 (left). Coefficients of capacity and electrostatic induction for three plate system of conducting plates of 18 μm x 18 μm dimensions. The cantilever metal rests on 0.5 μm of SiO$_2$, which defines the minimum separation $\zeta$ between cantilever and surface metals. (right) Calculated force applied on cantilever with and without consideration of oxide permittivity.

## 3. 2D FEM CALCULATIONS AND DESIGN OPTIMIZATION

The force can also be determined by integrating the negative electrostatic pressure $\varepsilon_0 E^2/2$ over the entire surface of the cantilever. We calculate the electric field distribution for a 2D model of the device using the finite element modeling software Elmer [8]. Since the calculation is 2D, the magnitude of the force is not quantitatively accurate for the actual 3D device, but the results are qualitatively informative. A 2D mesh was designed for a simplified 3-plate configuration (leaving out the oxide, the tip, and the legs) using Gmesh 2.7 [9]. The cantilever is given 100 nm thicknesses while surface plate and buried plate were considered as two dimensional sheets. The minimum mesh size is set to 100 nm to reveal any dependence on plate thickness.

Figure 3 presents the resulting spatial distribution of the vertical component of the electric field vector when all three plates have 10 μm dimensions [see electronic version for color]. Since the electric field is normal to a conductor surface, there are no horizontal electric-field components to consider, except at the ends, where the electric forces cancel by symmetry. The buried plate potential is set to -20 V while surface plate and cantilever are at +20 V. The field between surface and buried plate is strong and negative (downward). A negative fringe field extends to the bottom outer edges of cantilever, but the fields on top of cantilever are positive. The negative field below the cantilever drops to zero near the center while the positive field on top of the cantilever does not reach zero.

We stress that the sign of the field has no influence on the sign of the local electrostatic pressure $\varepsilon_0 E^2/2$, which is always outwards from the conductor surface. Thus, when mentally integrating over the surface of the cantilever from the image in Fig. 3, one should pay attention only to the magnitude of the field. Since this is larger over the top-surface of the cantilever than over its bottom surface, the net force is upwards.
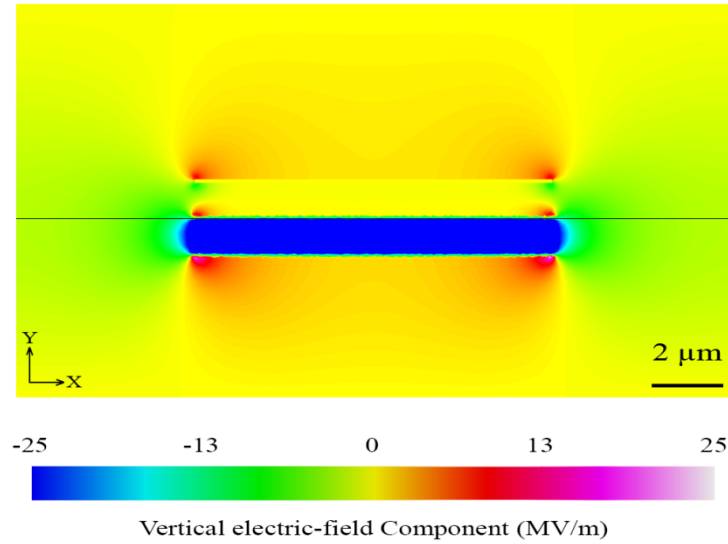
Figure 3. Electric field distribution of 10 μm long 3-parallel-plate system. Top and middle plates are at +20 V while the bottom plate is held at -20 V. Gaps between plates are 1 μm.

Field values are imported into Mathematica [10] for integration over the surface. Since fields peak near the edges, it is critical that all integrals have exactly the same limits. To ensure this, we perform a first order interpolation before integration. We then integrate the value of the negative electrostatic pressure $(1/2) \, \varepsilon_0 \, E^2$ over top and bottom cantilever surfaces to find the net electric force density in N/m.

Figure 4 (left) presents a plot of the total force density acting on the cantilever as a function of surface-plate length, holding the dimensions of the buried plate and cantilever constant. The separation $\zeta$ is also held constant at 1 μm. Figure 4 (inset) expands the cross-over region, where the force becomes positive (upward). This appears when the surface plate length is 95% of cantilever length, and it peaks at 105%.
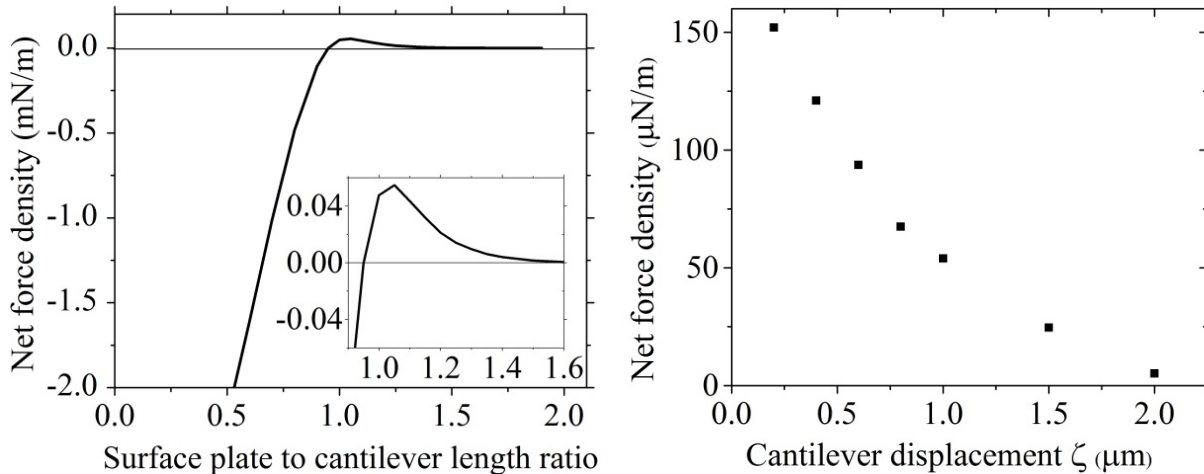


Figure 4. (left) Net force density vs. size of the surface plate relative to that of the cantilever. (right) Net force density vs. cantilever displacement.

Figure 4 (right) presents a plot of the net force density vs. the vertical separation $\zeta$ between cantilever and surface metals. The surface plate length was taken to be 5% larger than the others to achieve maximum net force, according to

Fig. 4 (left). Force density is plotted instead of force because these are results of a 2D calculation. The net force density approaches zero when $\zeta$ reaches 2 µm.

Figure 5 presents the spatial distribution for the vertical component of the electric field at $\zeta$ = 1 µm and 3 µm. As the height increases the negative fringing fields penetrate more into the space under the cantilever, while the positive field on top gets weaker. The net force eventually changes sign. Figure 5 (top) represents a situation with upward force on the cantilever. Fig. 5 (bottom) represents a downward force situation.
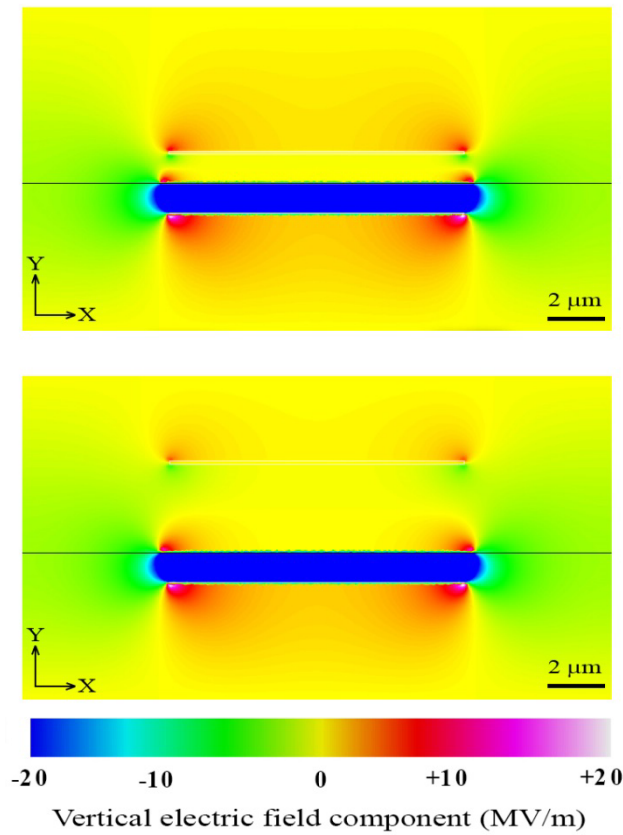


Figure 5. Distribution for the vertical component of the electric field vector (V/m) for z = 1 (top) and 3 µm (bottom). The dark line in the middle shows where substrate surface is located.

Since the field distribution is not uniform along the edge and stronger fields appear at the corners, force density results from 2D calculations cannot simply be multiplied by the plate's length to get total force on a 3D plate. The 2D model lacks two of the edges, which are the locations of highest charge density and surface fields (Figs. 3 and 5). Hence, these 2D calculations underestimate the magnitude of the force.

Figure 6 presents the net force as a function of surface plate to cantilever size ratio for the different cantilever heights indicated in microns next to each curve. For larger separations $\zeta$, the optimum ratio increases. The maximum achievable net force is a decreasing function of $\zeta$. To achieve positive force at larger separations requires a larger surface plate to screen the buried plate.
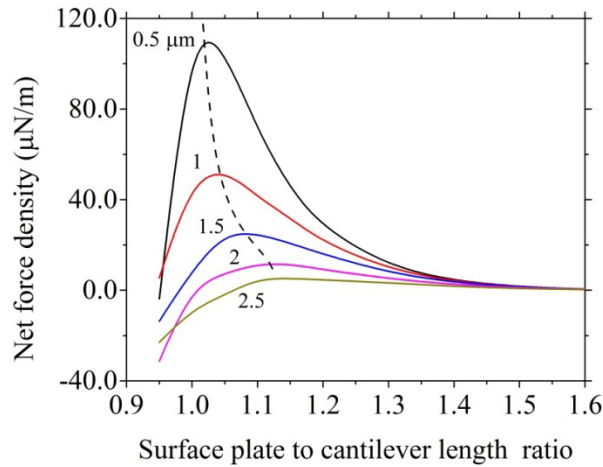
Figure 6. Force Density vs. surface plate to cantilever length ratio for different cantilever heights $\zeta$, whose values are indicated next to each curve in microns.

## 4. COMPARISON TO ELASTIC AND CASIMIR FORCES

Casimir force causes stiction between metal surfaces in MEMS devices [11]. It strongly depends on the separation between plates and becomes significant when this separation is very small. The electrostatic forces studied here can be generally useful in MEMS applications if they are able to overcome sticking forces. For proper function of the Edwards device [3], the upward electrostatic elastic force needs also to overcome the elastic restoring force, which tries to keep the tip of the cantilever in the null position.

The Casimir force for two square parallel plates of length L and separation $z$ is [12,13,14]

$$F = \frac{\pi^2 c \hbar L^2}{240 z^4} \qquad .$$  (2)

If the metal tip on the underside of the cantilever and the surface contact pad are both squares of dimensions 2 μm by 2 μm, the numerical value of the force is

$$F = \frac{5.2 \times 10^{-39} N m^4}{z^4} \qquad .$$  (3)

We have estimated the spring constant for the cantilever, assuming a pair of 18 μm x 2 μm x 0.4 μm oxide legs, to be 0.6 N/m [12]. Fig. 7 (left) compares the three forces in a log-log plot. The slopes of Casimir and Elastic forces are -4 and +1, respectively, as expected for power laws. The electrostatic force (including oxide permittivity, and using $z = \zeta - 0.5$ μm) is comparatively flat in this plot. For plate separations of less than 18 nm, the electrostatic force is unable to overcome the Casimir force. The situation is improved if the tip dimension is reduced to 25 nm, as shown in Fig. 4 (right). Then Casimir force will be less than electrostatic force for any gap higher than 2 nm. The average roughness of the surface of a commercial polished silicon wafer has this value, and it is unlikely that the two plates can be made parallel with this precision. Hence, we concluded that for sufficiently small tip, the electrostatic force can overcome the Casimir force.
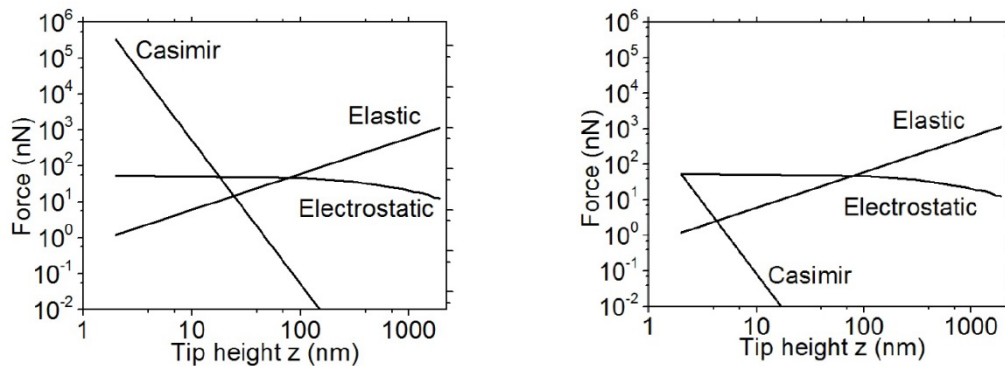
Figure 7. Casimir, elastic, and electrostatic forces for (left) 2 μm x 2 μm and (right) 25 nm x 25 nm tip dimensions.

## 5. SUMMARY

In this paper we have investigated vertical electrostatic force for a MEMS cantilever device consisting of three parallel metal plates. The cantilever plate is moveable and biased the same as a fixed surface plate, which is biased oppositely to a buried plate. The force on the cantilever is upwards, i.e. away from the surface. This force is maximized when the ratio of surface plate to cantilever dimensions is several percent greater than unity. Higher permittivity of the structural material gives stronger force. The electric force is compared to Casimir and elastic forces, and it was shown that sufficiently small tip allows the electrostatic force to lift the cantilever from the surface, if the contact distance is (on average) at least 2 nm. This method of achieving lift forces for MEMS devices is applicable to other types of devices such as micromirrors, switches, and sensors.

## 6. ACKNOWLEDGMENTS

## 7. REFERENCES

[1] Hu, F., Wang, W. and Yao, j. , "An electrostatic MEMS spring actuator with large stroke and out-of-plane actuation", J. Micromech. Microeng., 21 (11), 115029 (2011).
[2] Wang, W, Tao, F., Wang, Q., Qui, C., Chen, Z. and Yao, J., "A 19 Element Segmented MEMS Deformable Mirror Based on Electrostatic Repulsive-Force Actuator". Proc. SPIE 8617, 861702-1 (2013).
[3] Edwards, O., "Radiant energy imager using null switching", US patent 7977635 B2 (2011).
[4] Rezadad, I., Boroumand, J., Smith, E. M., Peale, R. E., "MEMS cantilever with electrostatically-controlled tip contact", Submitted to Appl. Phys. Lett. (2014).
[5] Boroumand Azad, J., Rezadad, I., Nath, J., Smith, E. and Peale, R. E., "Release of MEMS devices with hard-baked polyimide sacrificial layer", Proc. SPIE 8682, 868226 (2013).
[6] Javaneh Boroumand Azad, Imen Rezadad, Ammar Alhasan, Evan M. Smith, Robert E. Peale, "Thermomechancial characterization in a radiant energy imager using null switching", Proc. SPIE 9070 (2014).
[7] FastFieldSolvers S.R.L, Via de Castillia, 7, 20871 Vimercate (MB) Italy.
[8] CSC - IT Center for Science Ltd., P.O. Box 405, FI-02101 Espoo, Finland.
[9] Geuzaine, C. and Remacle, J.-F., "Gmsh: a three-dimensional finite element mesh generator with built-in pre- and post-processing facilities", International Journal for Numerical Methods in Engineering, 79(11), 1309-1331 (2009).
[10] Wolfram Research, Inc., Mathematica, Version 9.0, Champaign, IL (2012).
[11] Madou, M. J., [Fundamentals of Microfabrication and Nanotechnology], CRC Press, United States of America (2011).

[12] Alhasan, A., [Comparison of casimir, elastic, electrostatic forces for a micro-cantilever], Masters Thesis, UCF, Orlando ( 2014).
[13] Landau, L. D., Lifshitz, E. M., [Statistical Physics: Theory of the Condensed State], Butterworth-Heinemann, Oxford (1980).
[14] Casimir, H. B. G., Polder, D., "The Influence of Retardation on the London-van der Waals Forces" , Phys. Rev. 73, 360–372 (1948).